THE JOURNAL OF PHYSICAL CHEMISTRY B

Article

pubs.acs.org/JPCB

Probing the Conformationally Excited States of Membrane Proteins via ^{1}H-Detected MAS Solid-State NMR Spectroscopy

T. Gopinath,[†] Sarah E. D. Nelson,[†] Kailey J. Soller,[‡] and Gianluigi Veglia*[,†,‡]

[†]Department of Chemistry and [‡]Department of Biochemistry, Molecular Biology, and Biophysics, University of Minnesota, Minneapolis, Minnesota 55455, United States

ABSTRACT: Proteins exist in ensembles of conformational states that interconvert on various motional time scales. High-energy states of proteins, often referred to as conformationally excited states, are sparsely populated and have been found to play an essential role in many biological functions. However, detecting these states is quite difficult for conventional structural techniques. Recent progress in solution NMR spectroscopy made it possible to detect conformationally excited states in soluble proteins and characterize them at high resolution. As for soluble proteins, integral or membrane-associated proteins populate different structural states often modulated by their lipid environment. Solid-state NMR spectroscopy is the method of choice to study membrane proteins, as it can detect both ground and excited states in their natural lipid environments. In this work, we apply newly developed ^{1}H-detected ^{15}N-HSQC type experiments under moderate magic angle spinning speeds to detect the conformationally excited states of phospholamban (PLN), a single-pass cardiac membrane protein that regulates Ca^{2+} transport across sarcoplasmic reticulum membrane. In its unbound state, the cytoplasmic domain of PLN exists in equilibrium between a T state, which is membrane bound and helical, and an R state, which is membrane detached and unfolded. The R state is important for regulation of the sarcoplasmic reticulum Ca^{2+}-ATPase, but also for binding to protein kinase A. By hybridizing ^{1}H detected solution and solid-state NMR techniques, it is possible to detect and resolve the amide resonances of the R state of PLN in liquid crystalline lipid bilayers. These new methods can be used to study the conformationally excited states of membrane proteins in native-like lipid bilayers.

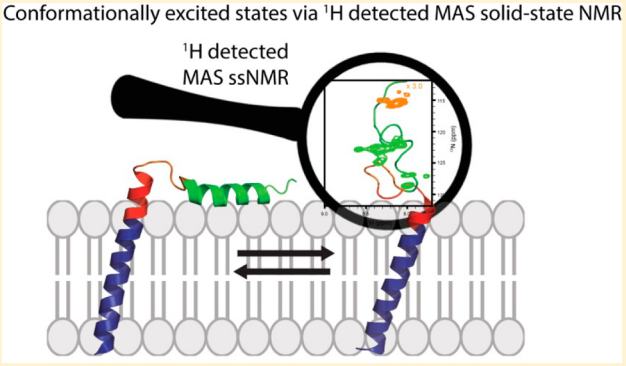

INTRODUCTION

NMR is a rapidly evolving technique for chemical, biochemical, and biophysical studies of macromolecules in solution, semisolid, and solid states. The most exciting frontier for NMR is to investigate membrane protein structures under physiological conditions, which has been very challenging for X-ray spectroscopy. Currently, both solution and solid-state NMR techniques are being used for studying membrane proteins. However, solution NMR is still limited to studying membrane proteins in detergent micelles, isotropic bicelles or in select cases, nanodisks, none of which are able to accurately mimic the composition of biological membranes. On the other hand, solid-state NMR (ssNMR) does not have a protein size limitation and is ideal for studying membrane proteins in native-like lipid membranes.[1−6] To maintain their tertiary fold and mimic proper functional conditions, membrane proteins need to be reconstituted in lipid membranes. Hydration, pH, temperature, lipid composition, as well as lipid-to-protein ratios, are crucial parameters to maintain transmembrane protein functional integrity.[7−9]

As with all biomacromolecules, membrane proteins exist as ensembles of low and high conformational energy states.[10] Biological responses to stimuli such as ligand binding, post-translational modifications, and changes in ionic or pH conditions skew the conformational equilibrium toward active or inactive states.[11] Often, biological activity is carried out by a high-energy conformational state (i.e., excited states) that is only sparsely populated under normal physiological conditions.[12] As both X-ray crystallography and cryoEM trap the structure of membrane proteins in defined, low energy basins, they cannot detect conformationally excited protein states. Using nuclear spin relaxation experiments, solution NMR experimentalists are able to detect protein and oligonucleotide excited states and determine their structures.[13−15] The presence of conformationally excited states is inferred through the analysis of protein motions. Although similar experiments have been proposed in ssNMR for microcrystalline protein preparations,[16] where solution-like properties of the spectra allow for measurement of $T_{1\rho}$ relaxation times, these methods are not readily applicable to membrane proteins within phospholipid membrane bilayers. In fact, the most important experiments for structure determination of membrane proteins

Received: April 6, 2017
Revised: April 13, 2017
Published: April 13, 2017

DOI: 10.1021/acs.jpcb.7b03268
J. Phys. Chem. B 2017, 121, 4456−4465

are based on cross-polarization (CP) techniques that rely on strong dipolar couplings (DC) for polarization transfer.[17] Although these approaches are now being combined with novel multidimensional acquisition methods,[18−20] they fail to detect dynamic regions that are likely to encode for conformationally excited states. The conformational plasticity of membrane proteins directly influences the magnitude of the orientational-dependent NMR interactions such as DC and chemical shift anisotropy (CSA).[21,22] As a result, dynamic regions of membrane proteins are insensitive to CP-based NMR techniques.[23] Certain regions of membrane proteins are also exposed to aqueous environments and undergo fast motions, thereby dramatically scaling down the dipolar interactions.[24] However, the conformational dynamics increase T_2 relaxation times of mobile residues enabling the application of through-bond INEPT (Insensitive nuclei enhanced by polarization transfer) experiments.[25] For instance, Baldus and co-workers have demonstrated the use of through-bond ^{13}C and ^{15}N detected refocused INEPT (RINEPT) experiments under MAS conditions for studying the cytoplasmic domain of the membrane protein phospholamban (PLN).[26] Similarly, ^{13}C detected RINEPT and CP experiments were respectively used for studying mobile and rigid domains of cartilage.[27] This approach has also been used for studying the dynamic regions of cytochrome-b5 using ^{15}N detected RINEPT experiment in oriented solid state NMR.[23,28,29] However, the intrinsic low sensitivity of ^{13}C and ^{15}N nuclei dramatically increases the experimental times.[30−34]

Recent progress in fast MAS experiments has enabled ^{1}H detection with dramatic sensitivity enhancement.[35−37] Perdeuterated sample preparations of crystalline proteins combined with ^{1}H detected fast MAS methods are now being routinely used for structure determination.[38] However, these methods have limited applications for membrane proteins reconstituted in phospholipid membrane mimetic systems. In this work we show that ^{1}H detected ssNMR can be used for studying dynamic regions of fully protonated membrane proteins at moderate MAS rates. We show that ^{1}H-detected ^{15}N HSQC-type MAS experiments are able to map the mobile residues of the conformationally excited state (R-state) of PLN under moderate spinning speed conditions. PLN is a 52-residue membrane protein that comprises an inhibitory transmembrane domain (domain Ib and domain II) and a regulatory domain (domain Ia), connected by a short, flexible loop (Figure 1A). PLN binds and regulates the sarcoplasmic reticulum Ca^{2+}-ATPase, or SERCA, decreasing its apparent affinity for Ca^{2+} ions in a reversible manner.[39] Protein kinase A recognizes and phosphorylates PLN at Ser16 in domain Ia, reversing this inhibition.[40] Previous solution and solid-state NMR as well electron paramagnetic resonance (EPR) experiments from our group and others[39,41,42] have shown that PLN's regulatory region in the absence of SERCA undergoes a conformational equilibrium between an ordered T state (helical) and a disordered R state (unfolded and membrane detached). The population of the R state was detected as weak peaks from the dipolar assisted rotational resonance (DARR)[43] experiments that mainly reported on the T state.[39] The application of the new refocused-INEPT heteronuclear single quantum coherence (RI-HSQC) pulse sequences enabled us to probe the R state of PLN with an average of 8-fold sensitivity enhancement compared to ^{15}N-detected INEPT-HETCOR experiments.[26] We also show that the sensitivity of these experiments is further enhanced by the simultaneous detection of cosine and sine

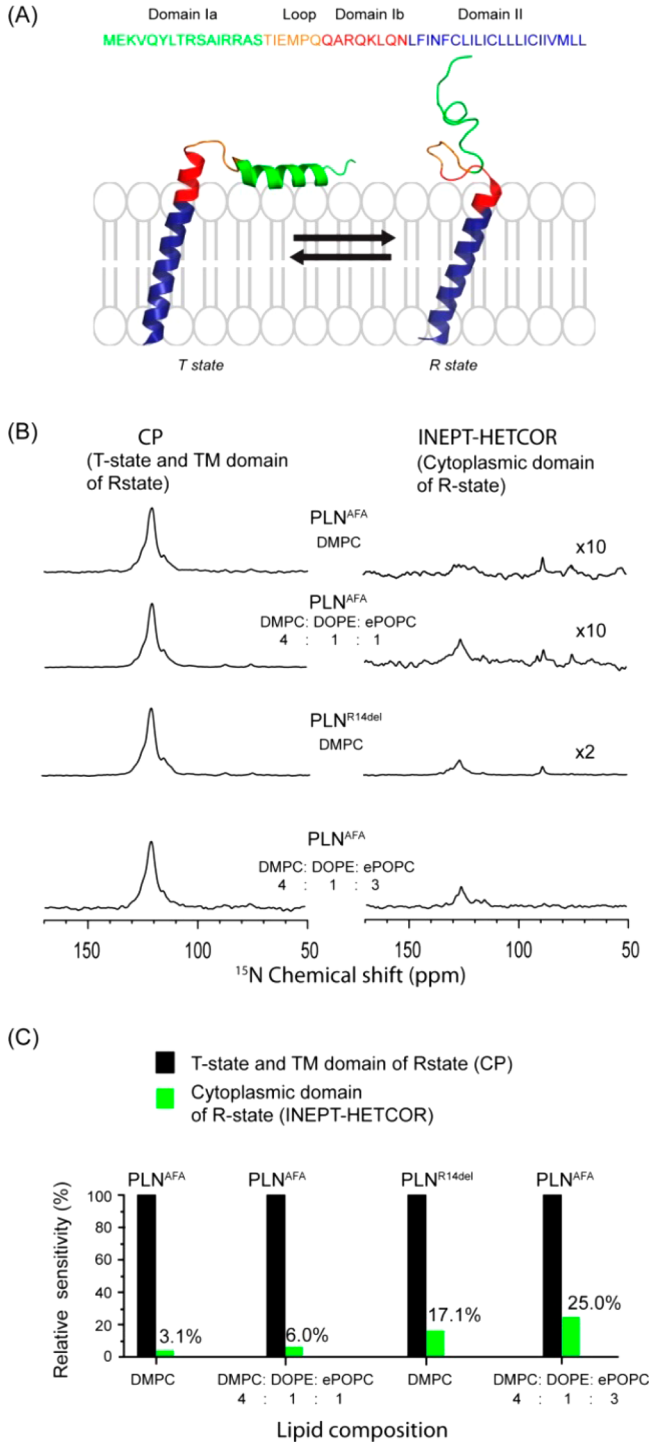

Figure 1. (A) Phospholamban conformational equilibrium between T (PDB 2KB7) and R (PDB 2LPF) states. (B) ^{15}N CP, and INEPT-HETCOR spectra of various PLN samples reconstituted in neutral DMPC or mixed DMPC, DOPE, and positively charged ePOPC lipid vesicles. (C) Relative sensitivity of INEPT-HETCOR spectra normalized with respect to CP is shown for each of the PLN samples reflecting the change in R-state population. Due to the complex interactions during CP and INEPT, this plot represents a relative estimation of the R state with respect to the T state.

modulated chemical shift coherences[44] with a new experiment called SERI-HSQC.

These new methods are applicable to a wide range of membrane proteins and complexes that display structural

DOI: 10.1021/acs.jpcb.7b03268
J. Phys. Chem. B 2017, 121, 4456−4465

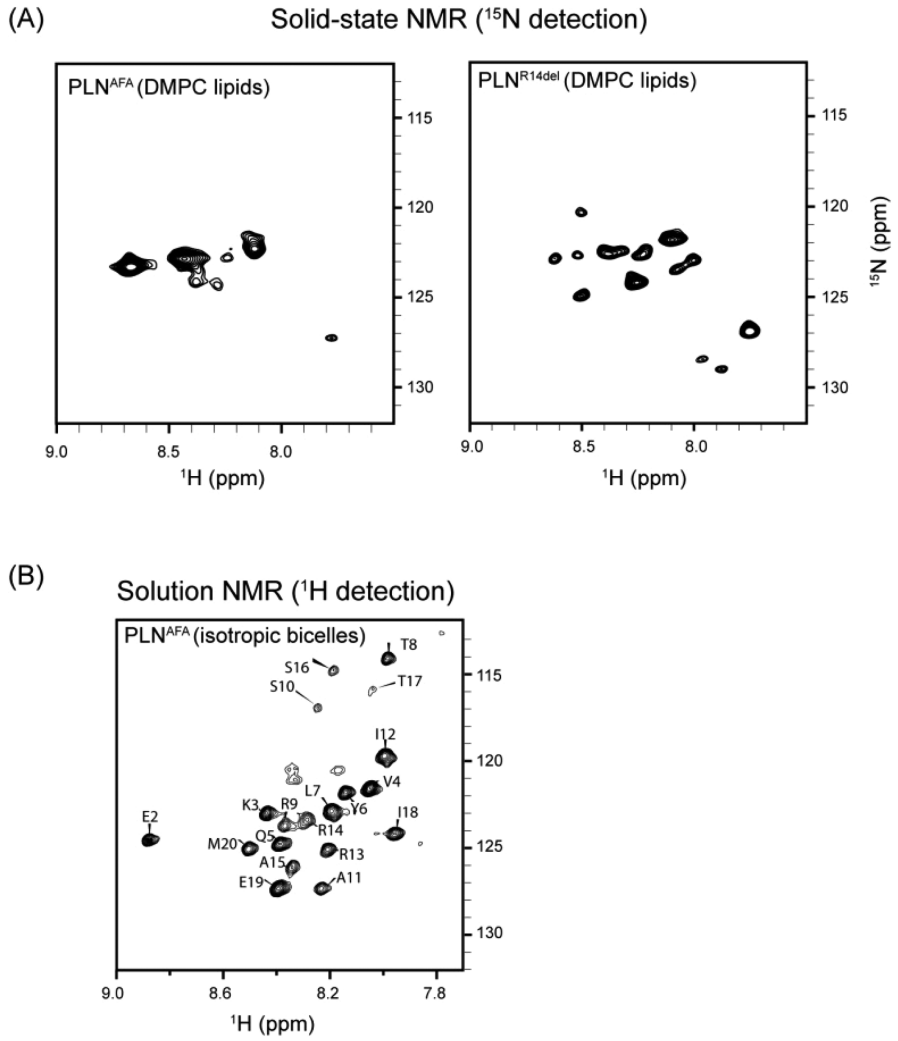

Figure 2. (A) Two-dimensional ^{15}N detected INEPT-HETCOR spectra that map the dynamic cytoplasmic domain of phospholamban membrane proteins (PLN^{AFA} and PLN^{R14del}) reconstituted in DMPC lipid vesicles. (B) Solution NMR HSQC spectrum of PLN^{AFA} reconstituted in isotropic bicelles, showing the assignment of cytoplasmic residues.

dynamic regions, allowing researchers to characterize their importance in biological function.

MATERIALS AND METHODS

Monomeric PLN (PLN^{AFA}) and R14 deletion PLN (PLN^{R14del}) were expressed in BL21(DE3) *Escherichia coli* and purified using affinity chromatography and HPLC according to the published procedures.[45] Purified PLN was lyophilized and stored at −20 °C. Protein reconstitution in lipid membranes and MAS sample preparations followed the previously published protocols.[39] Lipids for MAS samples were dried down under nitrogen and lyophilized once after resuspension in water to remove trace organic solvent. The lyophilized lipids were reconstituted in 2 mL of reconstitution buffer consisting of 20 mM HEPES (pH 7.0), 100 mM KCl, 1 mM $MgCl_2$, 5% (v/v) glycerol, and 0.02% (w/v) NaN_3. The lipids were solubilized using 25% $C_{12}E_8$, with 50 μL of detergent per 10 mg of lipid. PLN was solubilized in 25% $C_{12}E_8$, using approximately 25 μL per 1 mg of protein, and was added to the reconstituted lipid preparations. Following a brief incubation, BioBeads SM-2 were added in a 30-fold (w/w) excess over detergent and allowed to stir for 3 h at room temperature. The BioBeads were removed via filtration through a 25 gauge needle, and the lipid vesicles pelleted by centrifugation at 100 000*g* for 30 min at 4 °C. The pelleted vesicles were resuspended in 2 mL of the reconstitution buffer and centrifuged at 350 000*g* for 20 h at 4 °C. The resulting proteoliposomes were packed into 3.2 mm Bruker/Agilent MAS rotors using a series of centrifugation steps as previously described.[46] The final samples contained 0.5 to 2 mg of PLN reconstituted in neutral DMPC liposomes or charged lipid mixtures containing 4:1:1 or 4:1:3 ratios of DMPC:DOPE:ePOPC, where ePOPC is a positively charged lipid. All lipids were purchased through Avanti Polar Lipids and used without further purification.

All of the solid-state NMR experiments were acquired at the Minnesota NMR center using Bruker or Agilent spectrometers operating at a ^{1}H Larmor frequency of 700 MHz equipped with 3.2 mm probes with reduced RF heating technology.[47] All of the spectra were processed with 30 Hz line broadening, and 20k × 10k zero filling using NMRPipe,[48] and analyzed using Sparky.[49] For all ssNMR experiments, t_2 acquisition time was set to 100 ms for both ^{1}H and ^{15}N detections, 80 t1 points with 5 kHz t1 spectral width, and a recycle delay of 3 s. The PLN^{AFA} ssNMR spectra shown in Figures 2 and 8 were respectively acquired on Agilent spectrometer with 512 and 64 scans per t1 increment; whereas all of the remaining data were acquired on

DOI: 10.1021/acs.jpcb.7b03268
J. Phys. Chem. B 2017, 121, 4456−4465

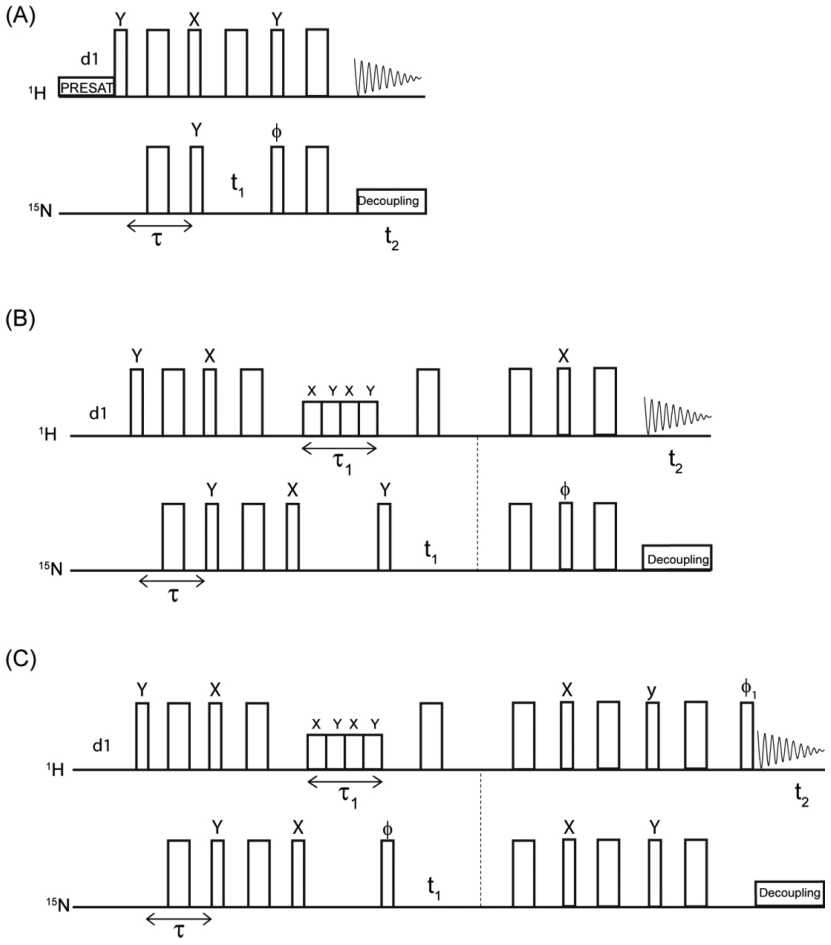

Figure 3. Two-dimensional ^{1}H−^{15}N correlation experiments for mapping the dynamical regions of membrane proteins using MAS solid-state NMR at moderate spinning speeds. Pulse sequences for HSQC (A), Refocused INEPT (RI) HSQC (B), and sensitivity enhanced (SE) RI-HSQC (C), with τ value set to 5.4 ms (=1/2J_{NH}). For HSQC, water suppression is obtained from a presaturation pulse during the recycle delay, whereas in RI-HSQC and SERI-HSQC RF spin locks during the τ_1 period (~250 ms) purges the water signal.[51] For all pulse sequences, a two-step phase cycle was used by switching the ϕ and receiver phases. For HSQC and RI-HSQC t_1 states acquisition was obtained by altering the phase of ϕ pulse between x and y, whereas for SERI-HSQC Rance-Kay mode t_1 acquisition was obtained by altering the ϕ_1 phase between x and $-x$.

Bruker spectrometer. The 90° pulse lengths for ^{1}H, ^{13}C, and ^{15}N were set to 3, 6, and 6 μs, respectively. For ^{1}H or ^{15}N heteronuclear decoupling, the WALTZ-16 sequence was used with the RF amplitude set to 10 kHz.[50] PLN^{R14del} spectra were acquired with 64 scans per each t1 increment. Water suppression in the HSQC pulse sequence was obtained from a continuous presaturation pulse during the recycle delay with RF amplitude set to 200 Hz. For both RI-HSQC and SERI-HSQC, spin-lock pulses with phases x and y were used with RF amplitude of 30 kHz and τ_1 set to 200 to 300 ms.[51] The RI-HSQC spectra of PLN^{AFA} in DMPC lipids was acquired with 1024 scans, whereas 600 and 400 scans were respectively used for mixed lipid samples 4:1:1 and 4:1:3 (Figure 6B). The heat induced at higher MAS rates was monitored by the water frequency of the ^{1}H spectrum, and compensated accordingly by lowering the sample temperatures. The spectra were indirectly referenced to the CH_2 resonance of adamantine sample at 40.48 ppm using the relative gyromagnetic ratio of ^{15}N and ^{1}H. Solution NMR HSQC spectrum of PLN^{AFA} in isotropic bicelles was recorded on 600 MHz spectrometer, using 128 scans and 64 t_1 increments with a total experimental time of 6 h.

RESULTS

Ground and Excited States of Phospholamban. In membranes, PLN undergoes a conformational equilibrium between an ordered T state (ground state) and a dynamic R state (conformationally excited state) as represented in Figure 1A. Our studies using PLN variants show that the population of these states can be shifted by phosphorylation, R14 deletion or by single site mutations.[39,52−55] At room temperature, it is possible to simultaneously observe both ground and excited states in slow exchange for selected resonances of the cytoplasmic domain using ^{13}C detected CP or INEPT based experiments. However, the resulting ^{13}C spectra are quite complex to analyze and typically require selective labeling.[39] Figure 1B shows the ^{15}N signatures for the backbone amides of the T and R states. These spectra were acquired using ^{15}N detection. While the more rigid residues of the transmembrane and membrane bound cytoplasmic domains are mapped by CP experiments, the more dynamic residues are observable using the relatively long J-coupling evolution periods (~10 ms) of the INEPT-based HETCOR experiment that selects for mobile residues with long T_2 relaxation time.[26] Therefore, in the CP spectrum it is possible to identify both transmembrane and membrane-bound cytoplasmic residues. On the other hand, the

DOI: 10.1021/acs.jpcb.7b03268
J. Phys. Chem. B 2017, 121, 4456−4465

INEPT-HETCOR experiment probes only cytoplasmic residues of the excited R state that undergoes fast conformational dynamics. A comparison of the 1D ^{15}N signal intensities at 25 °C for CP and INEPT- HETCOR spectra (Figure 1B,C) shows a significant difference in the relative R state population for the PLN^{AFA} and PLN^{R14del} variants reconstituted in neutral or fractionally charged mixed lipids. Figure 1C clearly demonstrates that while PLN^{AFA} in DMPC and 4:1:1 (DMPC:DOPE:ePOPC) mixed lipids exists primarily in the T state and is more sensitive to the CP-based experiment, deletion of R14, or increasing the percentage of positively charged lipids(4:1:3 mixed lipids), pushes the equilibrium toward the R state and increases the sensitivity of the INEPT-HETCOR experiment on these samples. Due to lower protein concentrations, CP and INEPT-HETCOR spectra of PLN^{AFA} were acquired using 10k to 50k scans. All the samples were acquired with identical experimental parameters. The integrated intensity of the CP and INEPT-HETCOR spectra were measured between 100 and 140 ppm at the same noise level. Although it is difficult to estimate the absolute R-state population, relative integrated intensity of INEPT-HETCOR with respect to CP indicates significant change in the relative R state population (Figure 1C). The latter is due to the decreased electrostatic interactions between the cytoplasmic domain and the membrane with the deletion of R14 or the introduction of positively charged lipids that shift the cytoplasmic domain toward the unfolded state due to an increase in PLN's conformational dynamics. The 2D INEPT-HETCOR spectra of PLN^{AFA} and PLN^{R14del} reconstituted in zwitterionic DMPC lipids are shown in Figure 2A. The number of peaks for PLN^{R14del} is higher than that of PLN^{AFA}, indicating more residues transition from the rigid, membrane bound T state to the more dynamic R state. For both samples, we observed significant variation in relative peak intensities as well as line widths between 45 to 105 Hz indicating different time scale motions of residues. Figure 2B shows the solution NMR HSQC spectrum of PLN^{AFA} reconstituted in neutral isotropic bicelles. Due to the longer correlation times of isotropic bicelles, immobile transmembrane residues are either weak or undetectable in this spectrum. Unlike in isotropic bicelles, PLN^{AFA} reconstituted in proteoliposomes shows very few peaks with significantly broader resonances (Figure 2A, top left), indicating a higher degree of conformational heterogeneity. This emphasizes that the motions of PLN^{AFA} cytoplasmic domain reconstituted in proteoliposomes are quite different from those in isotropic bicelles.

^{1}H-Detected MAS Solid-State NMR for Probing Excited States of Membrane Proteins. Although the ^{15}N-detected experiments are able to probe the R state confirmation for different PLN samples, we sought to boost sensitivity by using ^{1}H-detected HSQC experiments (Figure 3). A significant challenge for ssNMR is the suppression of the water signal in the ^{1}H detected spectra. While this is no longer a problem for solution NMR, where the probes are equipped with gradient coils and the water signal is easily dephased, commercially available ssNMR probes are not equipped with gradient pulse technology and deuterium spin-lock circuitry to compensate for the drift of the $\mathbf{B}_0$ field. In order to achieve reasonable water suppression, we used two modified pulse sequences, HSQC (Heteronuclear Single Quantum Coherence) and RI-HSQC (Refocused INEPT - Heteronuclear Single Quantum Coherence) that are similar to the solution NMR "out-and-back" experiments. For these HSQC-type experiments, the polarization transfer starts from ^{1}H to ^{15}N followed by ^{15}N t_1 evolution period and then is transferred back to ^{1}H for acquisition (t_2). Figure 3A shows the INEPT-based HSQC pulse sequence, where a presaturation pulse is applied on the water resonance during the recycle delay.[56,57] The second example of a pulse sequence utilizing ^{1}H detection is reported in Figure 3B. This experiment uses a refocused INEPT sequence to transfer the polarization from ^{1}H to ^{15}N which is then stored along the z-direction while suppressing (scrambling) the water magnetization using multiple pulses for a time period of τ_1 (~200 to 300 ms). After water suppression, a 90° pulse is applied on ^{15}N and is followed by a t_1 evolution period. A second refocused INEPT period is then used to transfer the ^{15}N polarization back to ^{1}H followed by t_2 acquisition period. The SERI-INEPT (sensitivity enhanced RI-HSQC) sequence shown in Figure 3C utilizes simultaneous detection of cosine and sine modulated chemical shift coherences to enhance the overall sensitivity and is explained further below.

Figure 4 shows the first increment of the ^{15}N and ^{1}H detected spectra of PLN^{R14del} in DMPC lipids at 25 °C using 12 kHz MAS rate and 64 scans. These spectra were obtained using

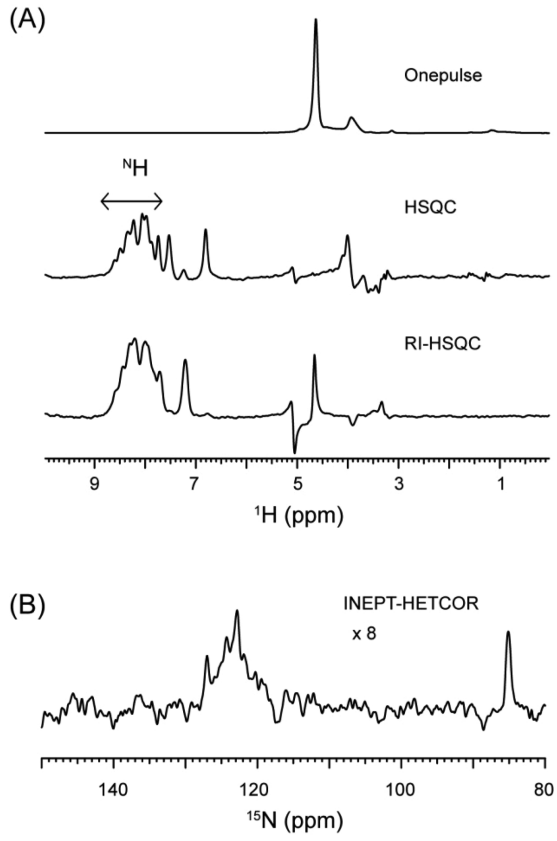

Figure 4. (A) Comparison of ^{1}H 1D spectra of PLN^{R14del} in DMPC lipids, obtained from one pulse experiment, and 1st increment (t_1 = 0) of ^{15}N HSQC and RI-HSQC. Efficient water suppression was obtained in HSQC and RI-HSQC displaying the amide proton spectra of protein. The net signal intensity in H^N region is about 25% lower for HSQC compared to RI-HSQC. (B) ^{15}N 1D spectrum obtained from INEPT-HETCOR experiment with t_1 = 0. The number of scans for acquiring HSQC, RI-HSQC, and HETCOR was set to 64. The sensitivity enhancement of RI-HSQC with respect to INEPT-HETCOR was approximately 10 times. Note that for the one pulse ^{1}H spectrum the receiver gain was lowered 10 times to avoid signal truncation.

DOI: 10.1021/acs.jpcb.7b03268
J. Phys. Chem. B 2017, 121, 4456−4465

HSQC, RI-HSQC, and INEPT-HETCOR pulse sequences with $t_1 = 0$. Although the 1D HSQC shows superior water suppression, the exchange between ^{H}N and water during the presaturation period lowers the signal intensity by ~25% in comparison to RI-HSQC. On the other hand, the ^{15}N 1D spectrum obtained from INEPT-HETCOR has nearly 10 times lower signal than the corresponding amide ^{1}H signal obtained from RI-HSQC. Unlike the HSQC and INEPT-HETCOR experiments, the duration of the RI-HSQC experiment is relatively longer, due to the water suppression period (τ_1) during which the ^{15}N magnetization is stored along the z-direction, and an additional 2τ period for in-phase coherence transfer between ^{15}N to ^{1}H. In spite of the longer duration of the RI-HSQC experiment, the gain in sensitivity is very significant with respect to both ^{15}N INEPT-HETCOR and ^{1}H HSQC.

To further enhance the sensitivity, we incorporated an additional τ period in the RI-HSQC sequence prior to t_2 acquisition according to the sensitivity enhancement scheme by Rance and co-workers.[58,59] The resultant pulse sequence, namely, sensitivity enhanced (SE) RI-HSQC (Figure 3C) simultaneously transfers both cosine and sine modulated ^{15}N coherences to ^{1}H and acquires the signals in a phase-sensitive mode by switching the ϕ_1 phase of ^{1}H pulse. The SE element nearly doubles the signal, whereas the RMS noise increases by 41% giving a theoretical sensitivity gain of 41%.

Figure 5 shows the 2D spectra of PLN^{R14del} reconstituted in DMPC lipids obtained from INEPT-HETCOR, HSQC, RI-HSQC, and SERI-HSQC experiments using 80 t_1 increments and 64 scans per increment. All the spectra were processed using 30 Hz line broadening in both dimensions. ^{1}H and ^{15}N line widths of resolved peaks are in the range of 45 to 105 Hz. The spectra of RI-HSQC, and SERI-HSQC were drawn at the same noise level, whereas the INEPT-HETCOR and HSQC spectra were multiplied by 8 and 1.3 times due to lower peak intensities. The average sensitivity of the 2D RI-HSQC is 10 times greater compared to the 2D INEPT-HECOR. In other words, a ^{15}N-detected INEPT-HETCOR experiment would require 100 times (10^2) more experimental time compared to RI-HSQC. As expected from the 1D spectrum, presaturation lowers the sensitivity of the 2D HSQC spectrum, causing some of the peaks in the 2D spectrum to have lower intensity with respect to the RI-HSQC. Interestingly, we also found that the ^{1}H line widths of HSQC are slightly narrower by 10 to 20 Hz compared to RI-HSQC. Most likely the narrower line widths in HSQC are due to presaturation pulse that eliminates the contribution of chemical exchange with water. The sensitivity of RI-HSQC is further enhanced by using SERI-HSQC, where the average sensitivity gain is 31% with respect to the RI-HSQC spectrum (Figure 5 bottom right panel).

Figure 6A demonstrates the sensitivity comparison of ^{1}H- and ^{15}N-detected spectra of PLN^{AFA} reconstituted in neutral DMPC lipids. In this case, the sensitivity of the 1D HSQC using presaturation is almost 3 times lower than the RI-HSQC spectrum. On the other hand, the 1D-HSQC shows dramatic signal enhancement for side chain resonances between 6 and 7.5 ppm, suggesting a possible increase of the magnetization due to NOE transfer taking place during presaturation. Figure 6B shows the comparison ^{1}H detected 2D RI-HSQC spectra of PLN^{AFA} reconstituted in DMPC or DMPC:DOPE:ePOPC lipid mixtures. The overall pattern of different spectra looks similar to small changes in peak positions or few additional peaks. Also, weak peaks of PLN^{AFA} were observed (between

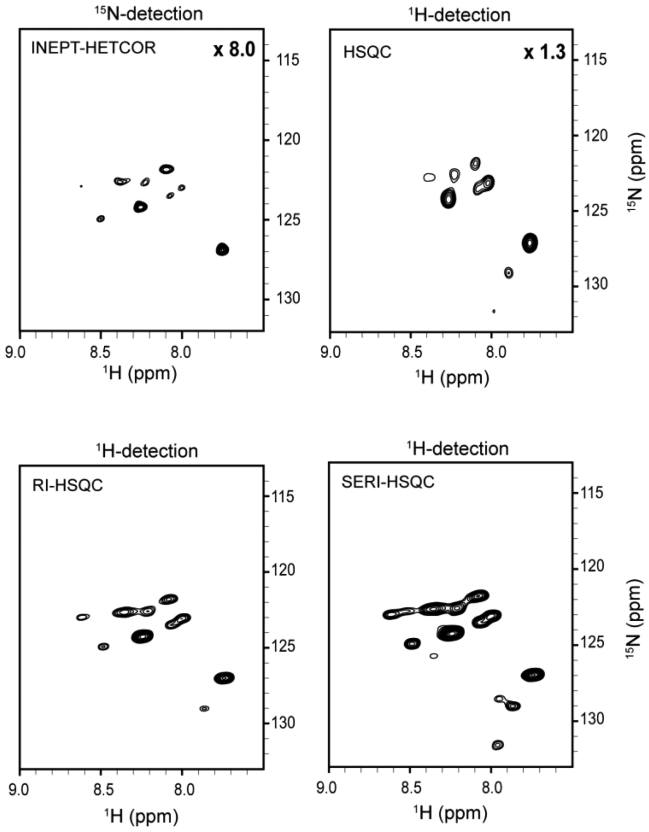

Figure 5. Two-dimensional ^{15}N–^{1}H correlation spectra of PLN^{R14del} in DMPC lipids, obtained from ^{15}N detection using INEPT-HETCOR, and ^{1}H detection using HSQC, RI-HSQC and SE-RI-HSQC pulse sequences. All the spectra were acquired using 64 scans and 80 t_1 increments. INEPT-HETCOR and HSQC spectra shown at 8 and 1.3 times higher noise floor. The relative integrated intensity of INEPT-HETCOR, HSQC, RI-HSQC, and SERI-HSQC between the spectral regions 7.5 and 9 ppm (^{1}H) and 113 and 133 ppm (^{15}N) is respectively 1.0:6.9:10.2:13.7.

112 to 117 ppm in the ^{15}N dimension) in mixed lipids samples, that were broadened when reconstituted DMPC lipids indicating more conformational heterogeneity. In fact these peak positions may correspond to Ser10, Ser16, and Thr17 residues (based on solution NMR assignment, Figure 2B) that were missing in the ^{15}N detected experiments (Figure 2A, top left) due to lower sensitivity. This also confirms that serine and threonine residues are less sensitive to through-bond polarization transfer indicating intermediate time scale motion.

Effect of Magic Angle Spinning Rate on Sensitivity and Resolution. The spinning speed can influence the appearance of the NMR spectra and high spinning speeds may in certain cases affect the sample stability. In order to understand the effect of spinning speed on sensitivity and resolution, we recorded the ^{1}H spectra using the RI-HSQC sequence at various MAS rates (Figure 7). While at 0 kHz broad peaks were observed, but the sensitivity was tremendously improved even at 5.5 kHz spinning speed. In fact for both the samples of PLN^{AFA} and PLN^{R14del} reconstituted in DMPC lipids, the gain in sensitivity is about 15 to 20% higher at 12 kHz compared to 5.5 kHz MAS rate. Whereas from 12 to 15 kHz, the gain in sensitivity is only about 2 to 5%. Figure 8 shows a comparison of the 2D RI-HSQC spectra of PLN^{AFA} in DMPC lipids at different spinning speeds. This indeed demonstrates that mobile residues in membrane proteins can

DOI: 10.1021/acs.jpcb.7b03268
J. Phys. Chem. B 2017, 121, 4456−4465

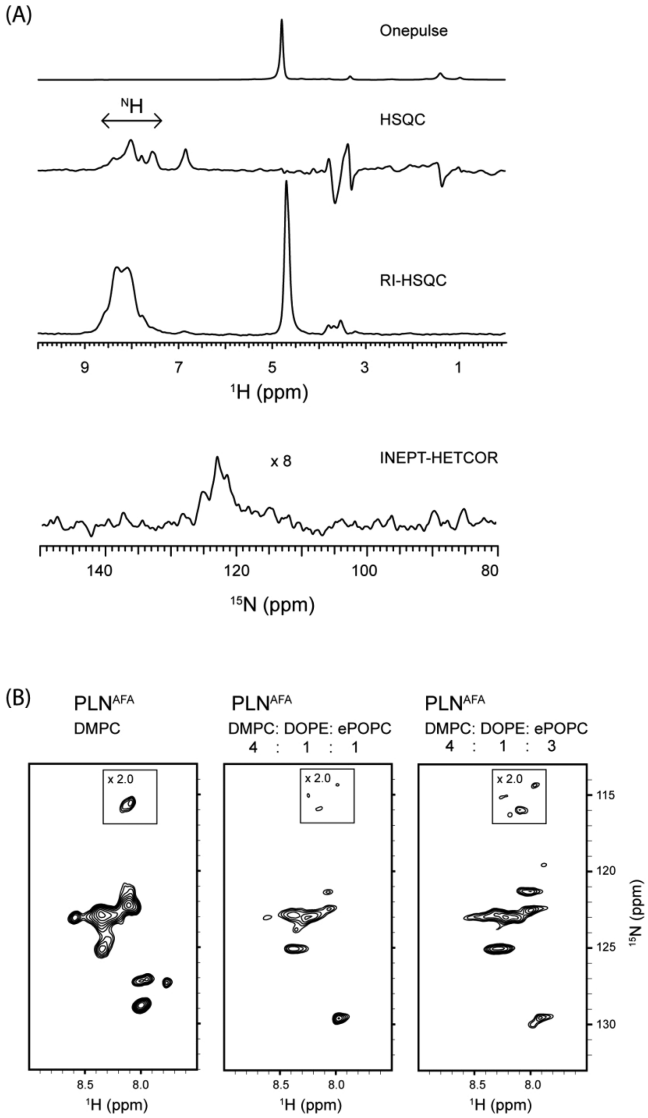

Figure 6. (A) HSQC, RI-HSQC, and INEPT-HETCOR 1D spectra of PLN^{AFA} in DMPC lipids, obtained from 2D pulse sequences with t_1 = 0. (B) Two-dimensional $^{15}N-^{1}H$ correlation spectra of PLN^{AFA} in various lipid compositions, obtained from ^{1}H detected RI-HSQC shown in Figure 3B.

be studied with optimal sensitivity and resolution using moderate spinning speeds via ^{1}H detection.

DISCUSSION

Both *in vitro* and *in vivo* studies indicate that in the monomeric form, PLN^{AFA} adopts an L-shaped conformation with the cytoplasmic domain undergoing a conformational equilibrium between T (bound) and R (free) states. The T state is helical and adsorbed on the surface of the bilayer, with the hydrophobic side chains pointing toward the interior of the membrane and the hydrophilic residues pointing toward the bulk solvent. On the other hand, the conformationally excited R state is membrane detached and unfolded. SERCA preferentially binds the R state with a helical conformation in the transmembrane domains and an extended conformation of the cytoplasmic domain.[39,60] Functional studies and mutations show that this conformational equilibrium is central to maintaining SERCA's Ca^{2+} transport within a physiological

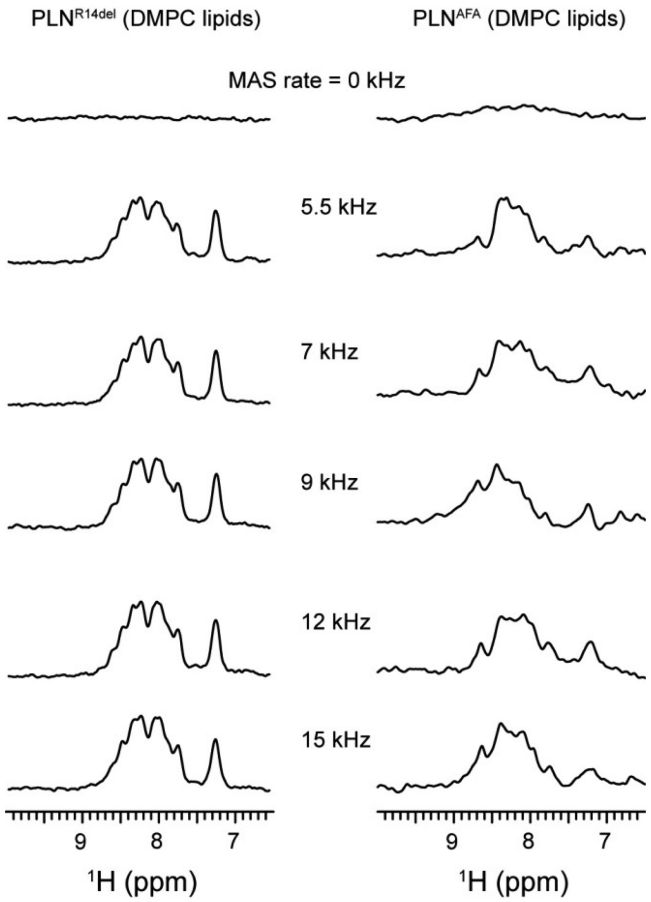

Figure 7. One-dimensional RI-HSQC spectra of PLN^{R14del} and PLN^{AFA} samples reconstituted in DPMC lipids. MAS rates were varied from 0 to 15 kHz. For both the samples, similar sensitivity enhancement was obtained as a function of MAS rate.

window.[52,54] In our previous studies, we showed that the population of dynamic R state, which can be biased by mutations, plays a major role in SERCA inhibition.[39,52] Additionally, the R state is the one selected by protein kinase A for phosphorylation.[61] Therefore, this high-energy conformational state plays a central role in PLN's regulatory function.

The R state of PLN^{AFA} was first detected by Baldus and coworkers using ^{13}C-detected through-bond correlations. Here, we show that ^{1}H-detected ^{15}N HSQC type experiments can probe dynamic regions of membrane proteins and provide higher sensitivity than ^{15}N-detected INEPT-HETCOR experiments. We demonstrated this with PLN's amide backbone fingerprint, which displayed a sensitivity increase up to 10 times higher than the corresponding ^{15}N-detected INEPT-HETCOR experiments. Though these new experiments will replace the highly insensitive ^{15}N detected experiments, it is important that new probes are developed containing gradients and lock circuitry since a significant hurdle is presented by the loss of sensitivity due to water exchange with backbone amide groups when applying presaturation of the water magnetization. Unlike solution NMR where the presaturation field strength is only about 50 Hz, we had to use ~200 Hz to cover larger spectral regions around the water frequency so that presaturation is still effective in spite of the $\mathbf{B}_o$ frequency drift. However, for insensitive samples, depending on the magnet drift, it is recommended to acquire multiple data sets with ^{1}H offset correction, which can then be combined for signal averaging.

DOI: 10.1021/acs.jpcb.7b03268
J. Phys. Chem. B 2017, 121, 4456−4465

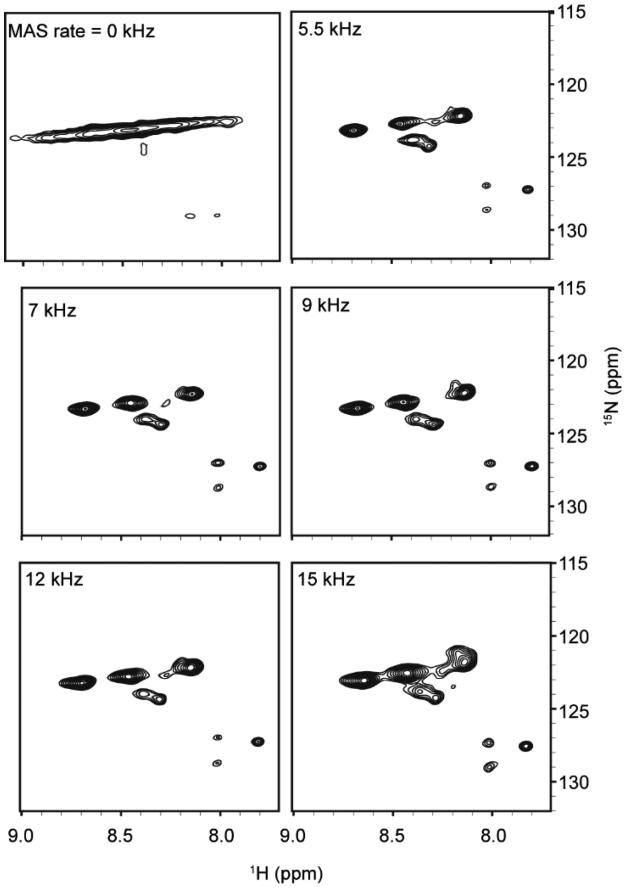

Figure 8. ^{1}H detected RI-HSQC spectra of PLN^{AFA} reconstituted in DMPC lipids, recorded from the pulse sequence of Figure 2B at various spinning speeds. All the spectra were drawn at the same noise level showing the relative sensitivity.

On the other hand, water suppression in RI-HSQC was obtained by applying a phase switched RF pulses on ^{1}H, while storing the ^{15}N magnetization along the *z*-direction. Therefore, water suppression in RI-HSQC and SERI-HSQC is insensitive to slight water frequency changes caused by the magnet drift. Water suppression can be avoided by reconstituting the protein in fully deuterated buffer. Recently, this approach was successfully used for studying mobile regions of *Anabaena* sensory rhodopsin using ^{13}C HSQC experiments at moderate MAS rates.[62] However, this method is limited to nonexchangeable aliphatic protons.[62] On the other hand, the RI-HSQC, and SERI-HSQC (Figure 3B,C) pulse sequences can be applied on fully protonated samples with 100% H2O, for studying labile amide protons. Interestingly, the loss of signal in the HSQC due to presaturation is higher for PLN^{AFA} compared to PLN^{R14del}. This indicates different ^{N}H−H_2O exchange rates of cytoplasmic domain in two different lipid systems. In fact, such experiments were used to study the exchange rates of globular proteins using solution NMR.[63]

Although current experiments were demonstrated using a regular MAS setup (without gradient and field lock channels) we anticipate a further gain in sensitivity and resolution with these technological advancements. In fact, double resonance (^{1}H−^{13}C) HR-MAS probes that are now routinely being used for metabolomics are equipped with gradient channels and deuterium spin-lock. While triple resonance HR-MAS probes could be promising for the detection of flexible domains or excited states of membrane proteins, they are limited to lower RF powers and MAS rates of 5 to 8 kHz.

CONCLUSIONS

In this study, we have shown that solid-state NMR is a unique method for probing ground and excited states of membrane proteins. Combination of CP and INEPT-based experiments were used to demonstrate the relative affinity of T and R states of PLN samples reconstituted in hydrated proteoliposomes. ^{1}H detected HSQC type experiments can be used under moderate MAS rates for mapping the excited states of membrane proteins or mobile residues of membrane proteins in fully hydrated lipid bilayers. These methods are demonstrated on PLN variants reconstituted in proteoliposomes, using commercial ssNMR probes without pulsed field gradients. Efficient water suppression was achieved by using RI-HSQC and detecting the amide protons with an average sensitivity enhancement of up to 10 times in comparison to ^{15}N detection. Incorporation of a sensitivity-enhanced element in the pulse sequence further enhances the sensitivity up to 40% using SERI-HSQC. Presaturation of water resonances in the HSQC pulse sequence leads to amide proton signal loss due to water exchange. In fact, the comparison of HSQC and RI-HSQC spectral intensity can be used for understanding water−protein interactions. Although these methods were demonstrated for 2D ^{15}N−^{1}H correlation experiments, it provides a basis for the development of 3D sequential correlation experiments for membrane proteins.

AUTHOR INFORMATION

Corresponding Author

*Mailing address: Department of Biochemistry, Biophysics, and Molecular Biology, University of Minnesota, 6-155 Jackson Hall, MN 55455. Telephone: (612) 625-0758. Fax: (612) 625-2163. E-mail: vegli001@umn.edu.

ORCID

Sarah E. D. Nelson: 0000-0001-6210-5009

Notes

The authors declare no competing financial interest.

ACKNOWLEDGMENTS

This research was funded by the National Institutes of Health (GM 64742 and GM 72701). All the NMR experiments were carried out at the Minnesota NMR Center. The authors would like to acknowledge Dr. V. Vostrikov and Dr. L. McDonald for their help in sample preparations and discussions.

REFERENCES

(1) Hong, M.; Zhang, Y.; Hu, F. Membrane Protein Structure and Dynamics from NMR Spectroscopy. *Annu. Rev. Phys. Chem.* **2012**, *63*, 1−24.

(2) McDermott, A. Structure and Dynamics of Membrane Proteins by Magic Angle Spinning Solid-State NMR. *Annu. Rev. Biophys.* **2009**, *38*, 385−403.

(3) Miao, Y.; Cross, T. A. Solid State NMR and Protein-Protein Interactions In Membranes. *Curr. Opin. Struct. Biol.* **2013**, *23*, 919−928.

(4) Salnikov, E. S.; Aisenbrey, C.; Aussenac, F.; Ouari, O.; Sarrouj, H.; Reiter, C.; Tordo, P.; Engelke, F.; Bechinger, B. Membrane Topologies of the PGLa Antimicrobial Peptide and a Transmembrane Anchor Sequence by Dynamic Nuclear Polarization/Solid-State NMR Spectroscopy. *Sci. Rep.* **2016**, *6*, 20895.

DOI: 10.1021/acs.jpcb.7b03268
J. Phys. Chem. B 2017, 121, 4456−4465

(5) Shahid, S. A.; Markovic, S.; Linke, D.; van Rossum, B. J. Assignment and Secondary Structure of the YadA Membrane Protein by Solid-State MAS NMR. *Sci. Rep.* **2012**, *2*, 803.
(6) Separovic, F.; Naito, A.; Price, W. *Advances in Biological Solid-State NMR: Proteins and Membrane-Active Peptides*; RSC Books: London, U.K., 2014.
(7) Zhou, H. X.; Cross, T. A. Influences of Membrane Mimetic Environments on Membrane Protein Structures. *Annu. Rev. Biophys.* **2013**, *42*, 361−392.
(8) Phillips, R.; Ursell, T.; Wiggins, P.; Sens, P. Emerging Roles for Lipids in Shaping Membrane-Protein Function. *Nature* **2009**, *459*, 379−385.
(9) Yamamoto, K.; Gildenberg, M.; Ahuja, S.; Im, S. C.; Pearcy, P.; Waskell, L.; Ramamoorthy, A. Probing the Transmembrane Structure and Topology of Microsomal Cytochrome-p450 by Solid-State NMR on Temperature-Resistant Bicelles. *Sci. Rep.* **2013**, *3*, 2556.
(10) Wei, G.; Xi, W.; Nussinov, R.; Ma, B. Protein Ensembles: How Does Nature Harness Thermodynamic Fluctuations for Life? The Diverse Functional Roles of Conformational Ensembles in the Cell. *Chem. Rev.* **2016**, *116*, 6516−6551.
(11) Kar, G.; Keskin, O.; Gursoy, A.; Nussinov, R. Allostery and Population Shift in Drug Discovery. *Curr. Opin. Pharmacol.* **2010**, *10*, 715−722.
(12) Mulder, F. A.; Mittermaier, A.; Hon, B.; Dahlquist, F. W.; Kay, L. E. Studying Excited States of Proteins by NMR Spectroscopy. *Nat. Struct. Biol.* **2001**, *8*, 932−935.
(13) Korzhnev, D. M.; Salvatella, X.; Vendruscolo, M.; Di Nardo, A. A.; Davidson, A. R.; Dobson, C. M.; Kay, L. E. Low-Populated Folding Intermediates of Fyn SH3 Characterized by Relaxation Dispersion NMR. *Nature* **2004**, *430*, 586−590.
(14) Neudecker, P.; Robustelli, P.; Cavalli, A.; Walsh, P.; Lundstrom, P.; Zarrine-Afsar, A.; Sharpe, S.; Vendruscolo, M.; Kay, L. E. Structure of an Intermediate State in Protein Folding and Aggregation. *Science* **2012**, *336*, 362−366.
(15) Xue, Y.; Gracia, B.; Herschlag, D.; Russell, R.; Al-Hashimi, H. M. Visualizing the Formation of an RNA Folding Intermediate Through a Fast Highly Modular Secondary Structure Switch. *Nat. Commun.* **2016**, *7*, ncomms11768.
(16) Ma, P.; Haller, J. D.; Zajakala, J.; Macek, P.; Sivertsen, A. C.; Willbold, D.; Boisbouvier, J.; Schanda, P. Probing Transient Conformational States of Proteins by Solid-State R(1rho) Relaxation-Dispersion NMR Spectroscopy. *Angew. Chem., Int. Ed.* **2014**, *53*, 4312−4317.
(17) Hartmann, S. R.; Hahn, E. L. Nuclear Double Resonance in the Rotating Frame. *Phys. Rev.* **1962**, *128*, 2042−2053.
(18) Wang, S.; Ladizhansky, V. Recent Advances in Magic Angle Spinning Solid State NMR of Membrane Proteins. *Prog. Nucl. Magn. Reson. Spectrosc.* **2014**, *82*, 1−26.
(19) Gopinath, T.; Veglia, G. Orphan Spin Polarization: A Catalyst for High-Throughput Solid-State NMR Spectroscopy of Proteins. *Annu. Rep. NMR Spectrosc.* **2016**, *89*, 103−121.
(20) Castellani, F.; van Rossum, B.; Diehl, A.; Schubert, M.; Rehbein, K.; Oschkinat, H. Structure of a Protein Determined by Solid-State Magic-Angle-Spinning NMR Spectroscopy. *Nature* **2002**, *420*, 98−102.
(21) Hu, F.; Luo, W.; Hong, M. Mechanisms of Proton Conduction and Gating in Influenza M2 Proton Channels from Solid-State NMR. *Science* **2010**, *330*, 505−508.
(22) Zachariae, U.; Schneider, R.; Briones, R.; Gattin, Z.; Demers, J. P.; Giller, K.; Maier, E.; Zweckstetter, M.; Griesinger, C.; Becker, S.; et al. beta-Barrel Mobility Underlies Closure of the Voltage-Dependent Anion Channel. *Structure* **2012**, *20*, 1540−1549.
(23) Xu, J.; Soong, R.; Im, S. C.; Waskell, L.; Ramamoorthy, A. INEPT-Based Separated-Local-Field NMR Spectroscopy: a Unique Approach to Elucidate Side-Chain Dynamics of Membrane-Associated Proteins. *J. Am. Chem. Soc.* **2010**, *132*, 9944−9947.
(24) Fusco, G.; De Simone, A.; Gopinath, T.; Vostrikov, V.; Vendruscolo, M.; Dobson, C. M.; Veglia, G. Direct Observation of the Three Regions in alpha-Synuclein that Determine its Membrane-Bound Behaviour. *Nat. Commun.* **2014**, *5*, 3827.
(25) Morris, G. A.; Freeman, R. Enhancement of Nuclear Magnetic Resonance Signals by Polarization Transfer. *J. Am. Chem. Soc.* **1979**, *101*, 760−762.
(26) Andronesi, O. C.; Becker, S.; Seidel, K.; Heise, H.; Young, H. S.; Baldus, M. Determination of Membrane Protein Structure and Dynamics by Magic-Angle-Spinning Solid-State NMR Spectroscopy. *J. Am. Chem. Soc.* **2005**, *127*, 12965−12974.
(27) Xu, J.; Zhu, P.; Morris, M. D.; Ramamoorthy, A. Solid-State NMR Spectroscopy Provides Atomic-Level Insights into the Dehydration of Cartilage. *J. Phys. Chem. B* **2011**, *115*, 9948−9954.
(28) Durr, U. H.; Yamamoto, K.; Im, S. C.; Waskell, L.; Ramamoorthy, A. Solid-State NMR Reveals Structural and Dynamical Properties of a Membrane-Anchored Electron-Carrier Protein, Cytochrome b5. *J. Am. Chem. Soc.* **2007**, *129*, 6670−6671.
(29) Huang, R.; Yamamoto, K.; Zhang, M.; Popovych, N.; Hung, I.; Im, S. C.; Gan, Z.; Waskell, L.; Ramamoorthy, A. Probing the Transmembrane Structure and Dynamics of Microsomal NADPH-Cytochrome P450 Oxidoreductase by Solid-State NMR. *Biophys. J.* **2014**, *106*, 2126−2133.
(30) Etzkorn, M.; Martell, S.; Andronesi, O. C.; Seidel, K.; Engelhard, M.; Baldus, M. Secondary Structure, Dynamics, and Topology of a Seven-Helix Receptor in Native Membranes, Studied by Solid-State NMR Spectroscopy. *Angew. Chem., Int. Ed.* **2007**, *46*, 459−462.
(31) Gao, M.; Nadaud, P. S.; Bernier, M. W.; North, J. A.; Hammel, P. C.; Poirier, M. G.; Jaroniec, C. P. Histone H3 and H4 N-terminal Tails in Nucleosome Arrays at Cellular Concentrations Probed by Magic Angle Spinning NMR Spectroscopy. *J. Am. Chem. Soc.* **2013**, *135*, 15278−15281.
(32) Renault, M.; Bos, M. P.; Tommassen, J.; Baldus, M. Solid-State NMR on a Large Multidomain Integral Membrane Protein: the Outer Membrane Protein Assembly Factor BamA. *J. Am. Chem. Soc.* **2011**, *133*, 4175−4177.
(33) Van Melckebeke, H.; Schanda, P.; Gath, J.; Wasmer, C.; Verel, R.; Lange, A.; Meier, B. H.; Bockmann, A. Probing Water Accessibility in HET-s(218−289) Amyloid Fibrils by Solid-State NMR. *J. Mol. Biol.* **2011**, *405*, 765−772.
(34) Yang, J.; Aslimovska, L.; Glaubitz, C. Molecular Dynamics of Proteorhodopsin in Lipid Bilayers by Solid-State NMR. *J. Am. Chem. Soc.* **2011**, *133*, 4874−4881.
(35) Mroue, K. H.; Nishiyama, Y.; Kumar Pandey, M.; Gong, B.; McNerny, E.; Kohn, D. H.; Morris, M. D.; Ramamoorthy, A. Proton-Detected Solid-State NMR Spectroscopy of Bone with Ultrafast Magic Angle Spinning. *Sci. Rep.* **2015**, *5*, 11991.
(36) Ravera, E.; Cerofolini, L.; Martelli, T.; Louka, A.; Fragai, M.; Luchinat, C. (1)H-detected Solid-State NMR of Proteins Entrapped in Bioinspired Silica: a New Tool for Biomaterials Characterization. *Sci. Rep.* **2016**, *6*, 27851.
(37) Zhang, R.; Pandey, M. K.; Nishiyama, Y.; Ramamoorthy, A. A Novel High-Resolution and Sensitivity-Enhanced Three-Dimensional Solid-State NMR Experiment Under Ultrafast Magic Angle Spinning Conditions. *Sci. Rep.* **2015**, *5*, 11810.
(38) Reif, B. Ultra-High Resolution in MAS Solid-State NMR of Perdeuterated Proteins: Implications for Structure and Dynamics. *J. Magn. Reson.* **2012**, *216*, 1−12.
(39) Gustavsson, M.; Verardi, R.; Mullen, D. G.; Mote, K. R.; Traaseth, N. J.; Gopinath, T.; Veglia, G. Allosteric Regulation of SERCA by Phosphorylation-Mediated Conformational Shift of Phospholamban. *Proc. Natl. Acad. Sci. U. S. A.* **2013**, *110*, 17338−17343.
(40) Kim, J.; Masterson, L. R.; Cembran, A.; Verardi, R.; Shi, L.; Gao, J.; Taylor, S. S.; Veglia, G. Dysfunctional Conformational Dynamics of Protein Kinase A Induced by a Lethal Mutant of Phospholamban Hinder Phosphorylation. *Proc. Natl. Acad. Sci. U. S. A.* **2015**, *112*, 3716−3721.
(41) Karim, C. B.; Kirby, T. L.; Zhang, Z.; Nesmelov, Y.; Thomas, D. D. Phospholamban Structural Dynamics in Lipid Bilayers Probed by a

DOI: 10.1021/acs.jpcb.7b03268
J. Phys. Chem. B 2017, 121, 4456−4465

Spin Label Rigidly Coupled to the Peptide Backbone. *Proc. Natl. Acad. Sci. U. S. A.* **2004**, *101*, 14437−14442.
(42) Yu, X.; Lorigan, G. A. Secondary Structure, Backbone Dynamics, and Structural Topology of Phospholamban and its Phosphorylated and Arg9Cys-Mutated Forms in Phospholipid Bilayers Utilizing 13C and 15N Solid-State NMR Spectroscopy. *J. Phys. Chem. B* **2014**, *118*, 2124−2133.
(43) Takegoshi, K.; Nakamura, S.; Terao, T. C-13-H-1 Dipolar-Assisted Rotational Resonance in Magic-Angle Spinning NMR. *Chem. Phys. Lett.* **2001**, *344*, 631−637.
(44) Gopinath, T.; Veglia, G. Sensitivity Enhancement in Static Solid-State NMR Experiments via Single- and Multiple-Quantum Dipolar Coherences. *J. Am. Chem. Soc.* **2009**, *131*, 5754−5756.
(45) Buck, B.; Zamoon, J.; Kirby, T. L.; DeSilva, T. M.; Karim, C.; Thomas, D.; Veglia, G. Overexpression, Purification, and Characterization of Recombinant Ca-ATPase Regulators for High-Resolution Solution and Solid-State NMR Studies. *Protein Expression Purif.* **2003**, *30*, 253−261.
(46) Mote, K. R.; Gopinath, T.; Veglia, G. Determination of Structural Topology of a Membrane Protein in Lipid Bilayers Using Polarization Optimized Experiments (POE) for Static and MAS Solid State NMR Spectroscopy. *J. Biomol. NMR* **2013**, *57*, 91−102.
(47) Gor'kov, P. L.; Chekmenev, E. Y.; Li, C.; Cotten, M.; Buffy, J. J.; Traaseth, N. J.; Veglia, G.; Brey, W. W. Using Low-E Resonators to Reduce RF Heating in Biological Samples for Static Solid-State NMR up to 900 MHz. *J. Magn. Reson.* **2007**, *185*, 77−93.
(48) Delaglio, F.; Grzesiek, S.; Vuister, G. W.; Zhu, G.; Pfeifer, J.; Bax, A. NMRPipe: a Multidimensional Spectral Processing System Based on UNIX Pipes. *J. Biomol. NMR* **1995**, *6*, 277−293.
(49) Goddard, T. D.; Kneller, D. G. *SPARKY* 3; University of Southern California: San Francisco, CA, 2001.
(50) Shaka, A. J.; Keeler, J.; Frenkiel, T.; Freeman, R. An Improved Sequence for Broadband Decoupling: WALTZ-16. *J. Magn. Reson.* **1983**, *52*, 335−338.
(51) Zhou, D. H.; Rienstra, C. M. High-Performance Solvent Suppression for Proton Detected Solid-State NMR. *J. Magn. Reson.* **2008**, *192*, 167−172.
(52) Ha, K. N.; Gustavsson, M.; Veglia, G. Tuning the Structural Coupling Between the Transmembrane and Cytoplasmic Domains of Phospholamban to Control Sarcoplasmic Reticulum Ca(2+)-ATPase (SERCA) Function. *J. Muscle Res. Cell Motil.* **2012**, *33*, 485−492.
(53) Ha, K. N.; Masterson, L. R.; Hou, Z.; Verardi, R.; Walsh, N.; Veglia, G.; Robia, S. L. Lethal Arg9Cys Phospholamban Mutation Hinders Ca2+-ATPase Regulation and Phosphorylation by Protein Kinase A. *Proc. Natl. Acad. Sci. U. S. A.* **2011**, *108*, 2735−2740.
(54) Ha, K. N.; Traaseth, N. J.; Verardi, R.; Zamoon, J.; Cembran, A.; Karim, C. B.; Thomas, D. D.; Veglia, G. Controlling the Inhibition of the Sarcoplasmic Ca2+-ATPase by Tuning Phospholamban Structural Dynamics. *J. Biol. Chem.* **2007**, *282*, 37205−37214.
(55) Vostrikov, V. V.; Soller, K. J.; Ha, K. N.; Gopinath, T.; Veglia, G. Effects of Naturally Occurring Arginine 14 Deletion on Phospholamban Conformational Dynamics and Membrane Interactions. *Biochim. Biophys. Acta, Biomembr.* **2015**, *1848*, 315−322.
(56) Kumar, A.; Ernst, R. R.; Wuthrich, K. A Two-Dimensional Nuclear Overhauser Enhancement Experiment for the Elucidation of Complete Proton-Proton Cross-Relaxation Networks in Biological Macromolecules. *Biochem. Biophys. Res. Commun.* **1980**, *95*, 1−6.
(57) Bax, A.; Ikura, M.; Kay, L. E.; Torchia, D. A.; Tschudin, R. Comparison of Different Modes of 2-Dimensional Reverse-Correlation NMR for the Study of Proteins. *J. Magn. Reson.* **1990**, *86*, 304−318.
(58) Kay, L. E.; Keifer, E.; Saarinen, T. Pure Absorption Gradient Enhanced Heteronuclear Single Quantum Correlation Spectroscopy with Improved Sensitivity. *J. Am. Chem. Soc.* **1992**, *114*, 10663−10665.
(59) Cavanagh, J.; Rance, M. Sensitivity Improvement in Isotropic Mixing (TOCSY) Experiments. *J. Magn. Reson.* **1990**, *88*, 72−85.
(60) Zamoon, J.; Nitu, F.; Karim, C.; Thomas, D. D.; Veglia, G. Mapping the Interaction Surface of a Membrane Protein: Unveiling the Conformational Switch of Phospholamban in Calcium Pump Regulation. *Proc. Natl. Acad. Sci. U. S. A.* **2005**, *102*, 4747−4752.
(61) Masterson, L. R.; Yu, T.; Shi, L.; Wang, Y.; Gustavsson, M.; Mueller, M. M.; Veglia, G. cAMP-Dependent Protein Kinase A Selects the Excited State of the Membrane Substrate Phospholamban. *J. Mol. Biol.* **2011**, *412*, 155−164.
(62) Ward, M. E.; Ritz, E.; Ahmed, M. A.; Bamm, V. V.; Harauz, G.; Brown, L. S.; Ladizhansky, V. Proton Detection for Signal Enhancement in Solid-State NMR Experiments on Mobile Species in Membrane Proteins. *J. Biomol. NMR* **2015**, *63*, 375−388.
(63) Spera, S.; Ikura, M.; Bax, A. Measurement of the Exchange Rates of Rapidly Exchanging Amide Protons: Application to the Study of Calmodulin and its Complex with a Myosin Light Chain Kinase Fragment. *J. Biomol. NMR* **1991**, *1*, 155−165.

DOI: 10.1021/acs.jpcb.7b03268
J. Phys. Chem. B 2017, 121, 4456−4465